CrystEngComm

Accepted Manuscript

Effect of additives on the large size growth of 4-N, N-dimethylamino-4-N-methyl stilbazolium naphthalene-2-sulfonate (DSNS) single crystal: An efficient stilbazolium derivative NLO crystal with potential Terahertz Wave properties

K.Senthil[a], S.Kalainathan[a]*, A.Rubankumar[a],

[a, a*]Centre for Crystal Growth, School of Advanced sciences, VIT University,
Vellore - 632 014, Tamilnadu, India.

[a]*Corresponding author

Prof.S.Kalainathan

VIT University, Vellore - 632014, Tamilnadu, India.

Phone: +91-416-2202350, Fax: 0416-2243092

E-mail Address: kalainathan@yahoo.com

Abstract

We explored the growth of the highly nonlinear optical stilbazolium salt 4-N, N-dimethylamino-4-N-methylstilbazolium naphthalene-2-sulfonate (DSNS) by slow evaporation method. The grown crystals are record size of crystals and exhibit the good optical quality. The harvested crystals have the suitable dimensions ~5 x 3mm^2 and the thickness in the range of 0.2-0.5mm^2 is reported for the first time by introducing the anionic additives STPB (Sodium tetraphenylborate) and DTPA (Diethylenetrimine pentaacetic acid anion) in the pure DSNS solutions. The grown crystals are highly suitable for fabrication of photonic devices and waveguiding applications. Through recrystallization of DSNS using various mixed solvents and conditions, we have obtained different crystalline phases. The grown crystals have been subjected to single crystal x-ray diffraction analysis to confirm the cell parameters. The crystallinity of the grown crystals was examined by using powder x-ray diffraction analysis. The various modes of functional groups present in the synthesized compound were confirmed using FT-IR and NMR spectral analysis. The transparency

range was analyzed using the UV-Vis-NIR spectral studies. The TGA/DTA analysis reveals the crystal is stable up to 300.2 °C.

1. Introduction

In recent years, the design of organic polar crystals with π-conjugated chromophores has attracted intensive attention because of large nonlinear optical susceptibilities compared with pure inorganic materials.[1-3] The large second harmonic generation (SHG) efficiency of organic salts are most often based on strong Coulomb interactions between appropriate electron donor and acceptor groups at the end of the π-conjugated structure.[4,5] However, the molecular nonlinearity is associated with orientation of π-chromophores in the crystal lattice. In addition, they have many advantages such as bulk non-linearity, long-term stability and a higher tendency to override the dipole-dipole interactions in the chromophores and thus form non-centrosymmetric structure.[6,7] Hence, intense efforts have been made worldwide to synthesis of extended π-conjugated system with donor and acceptor substituent because of their applications in the field of optical computing, telecommunication, high speed optical information processing, laser remote sensing, and laser frequency shifting applications. [8-10] A variety of organic nonlinear optical chromophores material (crystals) have been examined during the recent decade, it has been proved that the ionic organic crystals are of high concern because of their advantages in mechanical, chemical, superior long-term thermal, photochemical stability and orientation of ionic chromophore.[11-12] Among these compounds, DAST (4-dimethylamino-N-methyl-4-stilbazolium tosylate) is the most important one due to its large second-order nonlinear optical susceptibility (1000 times than that of the urea standard at 1907 nm) and electro-optic coefficient r11 of 77 pm V^{-1} at 800nm.[13-16] In the past few years, various crystal engineering techniques have been employed to control the morphology and improve the optical quality of DAST crystal.[17-19] For example, for integrated optic applications such as optoelectronics, photonics and THz wave's generation and detection, thin films with crystals having a thickness in the range of 0.1 mm to few mm scale are needed.[20-25] However, its bulk growth with sufficient optical quality crystal or thickness of DAST crystals remains a significant challenge. [26, 27] One of the promising stilbazolium DAST derivative with perfectly aligned chromophore is DSNS have been reported the powder SHG efficiency showed around 50% higher than DAST crystal at 1907 nm. They also demonstrated the growth of single crystal of DSNS approximately 2mm in length with a diameter less than 100 μm grown between two glass plates by slow evaporation method and the grown crystals observed between the crossed polarizers in a microscope was only reported to date. However, the growth of DSNS crystals is still a very challenging and is being investigated by many research groups worldwide the growth of thin films or bulk of DSNS.[28-30]

In this paper, large size single crystals of DSNS were successfully obtained by introducing additives such as STPB and DTPA adding in pure DSNS solutions. We have found that the rate of nucleation is reduced in the presence of additive in the solutions and also suppressing the clusters formation in the case of pure DSNS solution. The unit cell dimensions of the grown crystals were measured by a single crystal x-ray diffraction technique. The grown crystals of DSNS have been characterized by different instrumentation techniques such as powder X-ray diffraction (PXRD) analysis, spectroscopic analysis, optical absorbance, and thermal studies. Up to date, to the best of our knowledge, there is no report in the literature about DSNS to improve their growth by adding the effect of the organic additives and their characterizations. So far, we discuss these for the first time was described in detail.

2. Experimental methods

2.1 Material Synthesis. General considerations, all the necessary reagents, were purchased as high purity from Sigma-Aldrich, Alfa aesar and Merck Company. They were used without further purification. The overall synthesis process and reaction are illustrated in Scheme 1.

1, 4 Dimethylpyridinium Iodide 1. 1, 4 Dimethylpyridinium Iodide 1 was synthesized by equimolar ratio of 4-Picoline (2ml, 20mmol) and iodomethane (1.3ml, 20mmol) in acetone (30ml). The mixture solution was refluxed for 2 hours and cooled to ambient temperature. After removing the solvent and the salt dried at oven. The title salt *1* was obtained in quantitative yield.

4-[2-(4-Dimethylamino-phenyl)-vinyl]-1-methyl-pyridinium iodide 2. To the result of 1 (2.35g 10mmol) in hot methanol (30ml), 4-dimethylamino benzaldehyde (1.49g 10mmol), and piperidine (0.98ml, 10mmol) were added. The total above mixture was taken in the 250ml round bottom flask. Then the mixture solution was refluxed for 12 hrs under a dry nitrogen atmosphere. The resulting purple solid was filtered using a whatmann filter paper and three times washed with Diethyl ether for removal of unreacted starting materials. The title compound ***2*** was formed as a purple needle-shaped single crystals obtained by successive recrystallization from methanol by slow evaporation at ambient temperature. It had a melting point of 266 to 268°C.

DSNS. The mixture ***2*** (3.7g 10mmol) was dissolved in Millipore water (100ml) by heating. The hot aqueous solution of naphthalene-2- sulfonate (2.3g 10mmol) was added to the above solution. The above mixed solution was heated for 2 hours at 80°C and was cooled to ambient temperature. The red precipitate was filtered off and dried at 140°C for 1 hour by keeping the precipitate in hot air oven. The purity of DSNS was improved by repeated recrystallization by using methanol. The recrystallized high purity salt was used for the solubility studies and crystal growth.

2.2 Solubility Studies.

The solubility test plays a significant part in choosing the best solvent and temperature in the field of crystal growth. DSNS, whose chromophores are aligned perfectly parallel such a configuration, are of most interest for crystal growth experiments because it showed 50% larger SHG activity than DAST. However, its high potential for various applications, the growth of bulk size DSNS crystals has not yet been investigated in detail because it has not well soluble in most-polar solvents. In the present investigation, we have studied the solubility of DSNS using purified salt at different temperatures ranging from 30 to 45°C in five different combinations of solvents, namely methanol-chloroform (1:2), methanol-water (9:1), methanol-DMF (9:1), methanol-acetonitrile (1:1), and methanol-DMSO (9:1). The solubility study was carried out by dissolving the solute in 100ml of above said mixed solvent system in 150ml airtight containers. After that, the mixture was kept in an ultra-cryostat (UC) water bath maintained at 30°C, and the mixture was continuously stirred by using motorized magnetic stirrer to get the saturation. The UC stability is within ± 0.01°C. After attaining the equilibrium concentration of the solute solubility was determined by gravimetrically according to the following formula.

$$\text{Solubility (Wt\%)} = \frac{\text{Weight of the solute}}{\text{Weight of the (solute} + \text{solvent)}} \text{ x } 100$$

The same procedure was repeated to determine the equilibrium concentration of the solute with temperatures from 35°C to 45°C with 5°C interval. The solubility curves of pure DSNS with separate mixed solvent system at different temperatures are shown in Figure 1. From the graph, it can be observed that the solubility DSNS increase linearly with an increase of temperature.

3. Results and discussion

3.1 Crystal growth by different mixed solvent system.

Here, the crystallization experiments have been achieved in on a hot plate of heating energy controlled by energy regulator. To grow the single crystals of pure DSNS 500ml saturated solution was prepared according to its solubility diagram of DSNS at 45°C. Then the solution was continuously stirred with the help of magnetic stirrer to get the homogeneous and transparent solution. The prepared solutions were filtered by using a Whatman filter paper. After that, the filtered solution was evenly divided into five identical good quality borosil glass beakers (150 ml) with the help of a measuring jar. Again the beakers were covered tightly with aluminum foil with few holes and then placed on a hot plate, and the solutions were maintained at 50°C up to complete evaporation of the solvent by slow evaporation method. From this solvent system, many plate-like spontaneously has grown crystals were harvested from methanol-DMF (9:1) and methanol-DMSO (9:1) mixed solvent system. The low and high solubility of DSNS in methanol-water and methanol-chloroform mixed solvent system the crystallizations were absent due to low solubility of DSNS and fast evaporation of the solvent that in turn yielded only precipitation.

3.2 Effect of STPB and DTPA on crystal growth.

Plate-like single crystals of pure DSNS were grown in a mixed solvent system and obtained in the range of crystals approximately 0.5- 1.0mm thickness with different crystallographic faces from the slow evaporation method. However, in crystal engineering the morphology control is important for organic electro-optic crystals, which are very promising applications in imaging and terahertz (THz) wave generation and detection in terahertz time-domain spectroscopy (THz-TDS) applications. [31-33] In this investigation, nonpolar hydrophobic Teflon containers were used to avoid interface induced nucleation. In a glass container having hydrophilic surface, the nucleation first appears near the interface between air and evaporation-induced local supersaturation solution on the hydrophilic glass wall with surface interactions effect.[34] Considering the above problems during the DSNS crystal growth; we used Teflon containers to prevent the influence of effect. Therefore, the slow evaporation and slow cooling methods are suitable for the growth of DSNS crystal.

In this present research work, we examined the significance of beneficial effects of adding an additive on the growth rate of DSNS by the known concentrations of pure DSNS dissolved in methanol: acetonitrile (1:1) mixed solvent system. To grow bulk size crystals of DSNS, a known quantity of DSNS salt was dissolved in 100ml of methanol: acetonitrile (1:1) mixed solvent at 35°C with 20, 30 and 50ppm concentrations of STPB and DTPA added separately in the pure DSNS solutions. The resulting solution was continuously stirred for 2hrs in order to get the homogeneous saturation. Then the solution was filtered it using Whatman filter paper to remove extraneous solid. The additive added crystals were obtained by transferring filtered solution in Teflon beaker, which was tightly covered with aluminum foil with few holes. Optically transparent good quality single crystals of DSNS obtained by slow evaporation method for a period of 50-60 days from 50ppm of STPB and DTPA added pure DSNS solutions and for 20 and 40ppm yielded smaller crystals. Figure 2 shows the as-grown crystal of DSNS and different concentrations of STPB and DTPA added DSNS crystals. This small crystal size is a very attractive limit for the generation of high-power broadband THz waves. [35] The molecular structure of additives STPB and DTPA is given in Chart 1.

It has found that the additive added DSNS crystal is in higher growth rate, higher quality and with higher transparency. The addition of STPB and DTPA additives to the pure DSNS solutions are found to controlling the nucleation rate and suppress the crystal quality, inclusions by capturing metallic ions present in the solution with significantly compared to the pure one. The possibility of the commercially available chemicals has impurities of heavy metals like Ca^{+2}, Mg^{+2}, Pb^{+2},Cu^{+2}, etc. These impurities may induce the secondary nucleation and such impurities, having a long residence time in the adsorbed layer, become stoppers for the elementary steps and at higher supersaturations enhance the rate of heterogeneous nucleation on the surface. The distribution of metals becomes more difficult by the addition of additives has a high affinity to complex with metal cations, and the resulting complex does not enter and also prevents the entry of impurities into the crystal. Thereby good quality crystals are expected to grow for device applications.[36]

The additive incorporation also alters the nucleation time of the polymorphs in the solution. Due to the controlled evaporation of the solvent and the solution attains supersaturation and is responsible for nucleation as well as the growth promoting effect was also noticed in the presence of additives added DSNS solutions. Similar influence has also observed in the growth of DAST crystal.

3.3 Instruments for characterization

The single crystal lattice parameters of grown pure DSNS and STPB, DTPA added DSNS were obtained using a Bruker Kappa APEX II diffractometer with MoKα radiation (λ=0.71073Å) at room temperature. The grown single crystal was subjected to powder X-ray diffraction using a BRUKER X-Ray diffractometer with the CuKa radiation (λ=1.5406 Å), scanning angle ranges from 10 to 80° were used at a scan rate of 0.02°/s. The FT-IR spectra of the grown crystal have recorded in the range of 4000-400cm-1 by using SHIMADZU IRAFFINITY spectrometer by the KBr pellet method to verify the functional groups in the material. The optical transparency of the crystals was studied using an ELICO SL 218 double beam UV-Vis-NIR spectrophotometer in the region of 190-1100nm. In the present study, the formation of functional groups was identified from BRUKER-400MHz FT-NMR spectrometer using Dimethylsulfoxide (DMSO-d6) as solvent. The photoluminescence spectra of the sample were recorded by using F-7000 FL Spectrophotometer. The TGA/DTA study was carried out using NETZSCH STA-449F3 analyzer in the temperature range 25-500°C with a heating and cooling scan rate of 10°C/min in a nitrogen atmosphere.

3.4 X-ray diffraction analysis

Single crystal x-ray diffraction study has been carried out for the grown crystals to determine the lattice parameters, and to determine the crystal system. Table 1 represents the comparison of lattice parameters value of pure DSNS grown by using mixed solvent system and additive added

DSNS solutions, and these are in good agreement with the reported work by Blanca Ruiz et.al (CCDC- 292764).[28] The powder x-ray diffraction analysis has been also carried out for the grown crystals to analyze whether the title material is crystalline or amorphous. The x-ray diffraction pattern of pure DSNS and STPB, DTPA added crystals depicted in the Figure 3. No additional peaks were observed in the diffraction pattern of additive added DSNS crystal. Thus, it confirms that the added additives did not affect any change in the triclinic crystal structure of the DSNS crystal and did not induce a polymorphism, but significantly influenced the crystal morphology as shown in Figure 2. Thus, the observed prominent peaks confirm the good crystalline property of the grown DSNS crystals.

3.5 Density Measurement

The density measurement is one of the most-sensitive methods to evaluate the purity of crystals. The density of the crystals were measured by floatation method [37, 38] at room temperature (also called the swim or sink technique), and the obtained density values are presented in the Table 2. In this analysis, CCl_4 and was used as denser liquid and toluene was used as lower density liquid. For comparison, the density was also calculated using the crystallographic data

$$\rho = (MZ)/(NV),$$

where M is the molecular weight DSNS crystal (M=446.55 g/mol), Z is the number of molecules per unit cell (Z=1), V is the volume of the unit cell (V= 564.1 cm^3/unit cell), and N is the Avogadro number. Thus, the experimentally measured density is well-matched with the theoretically calculated values.

3.6 FT-IR Spectroscopic analysis

The recorded FTIR spectra for pure DSNS and the effect additive STPB and DTPA added DSNS crystals are depicted in Figure 4 (a-c). The band observed at 3392.79, and 3412cm^{-1} is typical for the OH stretching vibration in H_2O and which is due the moisture absorption from the air.

The peak at 3061.03 cm^{-1} is due to the aromatic C-H stretch. The band at 2914.43cm^{-1} is attributed to the alkyl C-H stretching mode. The peaks seen at 1629.85cm^{-1} are expected to C=C stretching mode of vibrations. The absorption peaks at 1591.27, 1558.48 and 1593.20, 1525.69cm^{-1} are assigned to the aromatic ring vibrations. The observed frequencies between 1438.90 and 1332.81cm-1 are due to the CH_3 bending absorption mode and C–N stretching mode. The band at 1193.94 and 1155.36 cm^{-1} is assigned to the symmetrically stretching vibration of SO_3 group.[39] The sharp peak at 962.48 and 999.13cm^{-1}is attributed to the vinyl =C–H stretching vibrations. Absorption wave numbers from 500 to 1000cm^{-1} are due to the substituent group of the aromatic ring vibrations. By comparing the graphs, (a) for the FTIR of pure DSNS crystal, (b) for STPB-added (c) for DTPA added DSNS crystal, there are no major shifts or additional peaks corresponding to STPB and DTPA added crystals compared to the pure crystal.

3.7 UV-Vis-NIR spectral analysis.

The optical absorption spectra of pure DSNS and STPB, DTPA added crystals were subjected to UV-Vis-NIR analysis by recording it in liquid form (dissolved in methanol) are depicted in Figure 5 (a-c). It was observed that the both pure DSNS and STPB, DTPA added DSNS crystals gives two peaks along with a large transmission in the Vis-NIR region, which is one the most-desired properties for applications in the red and near IR wavelength range and better photostability applications.[40] From the obtained spectrum, the minor peak at near 271 nm is corresponding to n- π* transition and another one is found around at 476nm represents the π-π* transition. The observed major absorption peak 476nm is due to the stilbazolium chromophore. The λ_{max} values in the UV-Vis-NIR spectra of above results indicate that there is no addition peak found in the case of adding an additive in pure DSNS electronic structure. Thus, the absorption behavior of additive added DSNS solutions shows the cutoff wavelength in the visible range is in good agreement with pure DSNS in the solutions phase. The λ_{max} value of DSNS is compared with a few other stilbazolium derivatives are listed in Table 3.

3.8 ^{1}H NMR and ^{13}C NMR Spectral studies.

The ^{1}H NMR and ^{13}C NMR spectral analysis were made on the powder form of pure DSNS crystal was recorded by dissolving it in DMSO-d6 as solvent. Figure 6 shows the ^{1}H NMR spectrum of pure DSNS crystal. The singlet at 3.019ppm and 8.14ppm is assigned to six N-$(CH_3)_2$ hydrogens and one of $C_{10}H_7SO_3$ hydrogen's. The singlet lies at 4.169ppm is expected to the three protons in the N-CH_3. The observed singlet at 3.367ppm and quintet signal at 2.514ppm are assigned due to the water molecule in DMSO-d6 and DMSO-d6 solvent. The doublet at 7.180ppm is expected to the two olefinic hydrogen's (CH=CH). The doublet at 6.794ppm and 7.701ppm is assigned due to the four hydrogen's of the N-$(CH_3)_2$-C_6H_4 in the aromatic ring. The multiple at 7.524 ppm is corresponding to the two hydrogens of the naphthalene ring (2H-C_{10} H_7 SO_3).[28] The doublet at 8.041, 8.68ppm, and 7.726ppm are assigned due to the four hydrogens of the N-C_6H_4 pyridinium ring and one hydrogen of a naphthalene ring. The multiple peaks observed at 7.985ppm, and 7.849ppm is attributed the four hydrogens in the naphthalene ring (4H- $C_{10}H_7$+CH). ^{13}C NMR spectrum of pure DSNS crystal is shown in Figure 7. The signal at 18.53, 46.32 and 56.01 ppm indicate that the presence methyl group carbon in pure DSNS. There are nine peaks 132.12, 130.11, 117.10, 144.31, 111.92, 145.64, 132.68, 123.98 and 153.33ppm, which are due to the stilbazolium moiety. The naphthalene-2- sulfonate ring carbons were identified at 126.36, 127.42, 141.86, 126.26 and 122.43ppm. Thus, the NMR spectral analysis confirmed the formation the title compound.

3.9 Photoluminescence studies.

Photoluminescence (PL) spectral analysis is a one of the nondestructive method to provide the electronic structure of materials and also widely used to identify the impurities and finds applications in lighting technologies. Luminescence properties may expect in compound containing aromatic structure with extended conjugated double bonds with a high degree of the resonance stability exhibits luminescence. [42, 43] Luminescence materials find extensive applications in branches of biological and biomedical science, and chemical research fields, for analyzing organic compounds.[44] The emission spectra of pure DSNS were carried out at room temperature using an F-7000 FL Spectrophotometer, in the scanned wavelength range between 530 - 820nm. For this emission spectrum, the excitation wavelength was used for this sample is 476nm from the UV spectral studies. The recorded PL spectrum of pure DSNS is given in Figure 8. The recorded spectrum consist two peaks in the visible region, and one is high-intensity emission peak at 2.03 eV (608nm) and followed another one is medium intense peak wavelength at 1.84 eV (665nm). It may do due the anionic and cationic group present in DSNS crystal matrix. From this wavelength, it covers the red emission in the visible region concluded that DSNS has a red luminescence emission. Thus, it may suggest that DSNS is most useful for near-infrared optical switching applications.

3.10 TGA/DTA Analysis.

Figure 9 shows the thermo gravimetric analysis (TGA) and differential thermal analysis (DTA) response curves of pure DSNS powder sample. The initial mass of the powdered crystal subjected to the analyses was 1.20 mg. The TGA curve shows that loss of weight of about 2.90% between 30 and 246 °C. This indicated that removal of water and evaporation of volatile substances during this temperature range. The DTA trace gives one sharp endothermic at 300.2°C, which is corresponding to the melting point of DSNS crystal. The sharpness of this endothermic peak illustrates the good degree of crystallinity and purity of the crystal. After melting, there are two endothermic peaks are observed around at 353.93 °C and 413.81°C. This indicates that complete decomposition of the stilbazolium ion from DSNS. In the TGA spectrum, there is a significant weight loss of about 33.34% starting at 307.22 °C and it continuous up to 364.10 °C. There is another 31.23% weight loss up to 549.50 °C. These weight losses are due to complete decomposition of the DSNS and release of SO_3. The final residue weight left over after a major weight loss was about 32.52% remains as carbon residue, which is present in the DSNS material at 550 °C. Based on this study, it is concluded that the crystal is thermally stable up to 300.2 °C and greater than DAST and its derivatives. The melting point of DSNS is comparison with some stilbazolium derivatives crystals with promising NLO materials was listed in Table 4.

4. Conclusions

We have investigated the growth of DSNS crystal by mixed solvent system and adding of additives STPB and DTPA in pure DSNS solutions. It has been noticed that enhanced the growth rate of the crystals as well as effectively change the crystal morphology while increasing the concentration of additives compared to the pure DSNS. It may be due to suppressing the activities of the metal ions present in the solution. The refined single crystal XRD results confirm that there is no incorporation of additives in the grown crystal structure. The solubility of DSNS in several mixed solvents system was estimated by the gravimetric method. From the solubility measurements, it is found that methanol: acetonitrile (1:1) mixed solvent was suitable for the growth process. The FTIR spectral analysis confirm that the presence of functional groups in the grown crystals. The UV–Vis-NIR spectral studies reveal that the low cutoff wavelength and there is no absorption in the entire visible region (476 -1100nm), and also no extra phase in absorption window for additive added crystals as compared to that of pure crystal. The good transparency of the pure and additive added DSNS crystal in the entire Vis-NIR region ensures its suitability for NLO device fabrication. Luminescence studies exhibit that the DSNS crystal has red luminescence emission property. The melting and decomposition temperature range of the grown single crystal has been studied from TGA/DTA analysis, and it reveals the purity and the crystals show an improved thermal stability up to 300.2 °C, compared to DAST and its derivatives crystals. Based on the obtained results, we conclude that the additives played a drastic role in the changes of the growth process and the morphology (shape) of the DSNS crystals and also noticed that there is no incorporation of STPB or DTPA in the DSNS molecular structure. Future investigations to this extent for various applications are in progress and will be our future publication. Thus, the obtained results which will in turn the scientific community and introduce the efficient method of growing high-quality DSNS crystal and its derivative crystals in the development of opto-electronic industry.

Acknowledgment.

We gratefully acknowledge financial support of this research by Defense Research and Development Organization (DRDO), Government of India for financial assistance. The authors are grateful for the management of VIT University, Vellore for their excellent research facilities and constant support and encouragements.

References

1 Li. Zhengdong, Wu. Baichang, Su, Genbo, *J Cryst. Growth,* 1997,178, 539.

2 L. Mutter, F.D. Brunner, Z. Yang, M. Jazbinsek, P. Günter, *J. Opt. Soc.*, 2007, 24, 2556.

3 Z.Yang, L. Mutter, B. Ruiz, S.Aravazhi, M. Stillhart,M. Jazbinsek,V.Gramlich,P. Günter, *Adv. Funct. Mater.*, 2007, 17, 2018.

4 N. Ritesh, Sethuraman, S. Beilstein, *J. Org. Chem.*, 2010, 6, 992–1001.

5 S. Shahab Naghavi, G.Thomas, A. Vajiheh, H.F. Gerhard, F.Claudia, M. Katerina, K. Dmytro, A.N. Sergej, S. Gerd, R. Ralph, B. Martin, M.J. Klaus, *Mol. Spectrosc*., 2011, *265*, 95–101.

6 B.J. Coe, J.A. Harris, I. Asselberghs, K. Wostyn, K.Clays,A. Persoons, B.S. Brunschwig, S.J. Coles,T. Gelbrich, M.E. Light, M.B. Hursthouse,K. Nakatani, K. *Adv. Funct.Mater*., 2003, *13*, 347.

7 D.J. Williams, *Ang. Chem. Int. Ed. Engl*., 1984, *23*, 690.

8 M. Iwai, T. Kobayashi, H. Furuya, Y. Mori, T. Sasaki,*J. Appl.Phys*., 1997, *36*, 276.

9 M. S. Wong, C. Bosshard, F. Pan, P. Gunter, *Ad. Mater.,* 1996, *8*, 677-680.

10 I. Ledoux, *Synth. Met*., 1993, *54*, 123.

11 B. J. Coe, J. A. Harris, A.K. Clays,G. Olbrechts,A. Persoons, J. T. Hupp, R.C. Johnson, S.J. Coles, M.B. Hursthouseand, K. Nakatani, *Adv. Funct. Mater*., 2002, *12*,110.

12 Li. Liang, Huijuan Cui, Zhou Yan, Xutang Tao, Xinsong Lin, Ning Ye, Huai Yang, C*rystEngComm*, 2012, 14, 1031–1037.

13 S. Sohma, H. Takahashi, T. Taniuchi, H. Ito, *Chem. Phys*., 1999,245, 359.

14 S.R. Marder, Perry, J.W. Schaefer, W.P. *Science*, 1989, 245, 626.

15 G. Knopfle, R. Schlesser, R. Ducret, P. Gunter, *Nonlinear Opt*., 1995, 9, 143.

16 F. Pan,G. Knopfle, C. Bosshard, R. Spreiter, M.S. Wong, P. Gunter, *Appl. Phys. Lett,.* 1996, 69, 13.

17 T. Matsukawa, Y. Mineno, T. Odani, S. Okada, T. Taniuchi, H.J. Nakanishi, *J. Cryst. Growth,* 2007, 299, 344.

18 M. Stillhart, A. Schneider, P. Gunter, *J. Opt. Soc. Am.,* B2008, 25, 1914

19 L. Mutter, F.D.J. Brunner, Z. Yang, M. Jazbinsek, P. Gunter, *J. Opt. Soc. Am.,* B2007, 24, 2556.

20 A.M. Sinyukov, L.M.J. Hayden, *Phys. Chem.,* B2004, 108, 8515.

21 D. Dragoman, M. Dragoman, Prog. *Quantum Electron.,* 2004, 28, 1.

22 M. Walther, B.M.Fischer, A. Ortner, A. Bitzer, A. Thoman, H. Helm, *Anal. Bioanal. Chem.,* 2010, 397, 1009

23 A.Schneider, M. Stillhart, P. Gunter, *Opt. Express.,* 2006, 14, 5376.

24 P.J. Kim, J.H. Jeong, M.K. Jazbinsek, S.J. Kwon, H. Yun, J.T. Kim, Y.S. Lee,I.H. Baek, F. Rotermund, P. Gunter, O.P. Kwon, *CrystEngComm.,* 2011, 13, 444.

25 E.Y.Choi, J.Y. Seo, M. Jazbinsek, O.P.Kwon, *Cryst. Growth Des.,* 2009, 9, 4269.

26 M.Thakur, J. Titus,A. Mishra,*Opt. Eng.* 2003, 42, 456.

27 A. Haja Hameed, W. Yu, Z. Chen, C. Tai, C. Lan, *J. Cryst.Growth.* 2005, *282*, 117.

28 Blanca Ruiz, Zhou Yang, Volker Gramlich, Mojaca Jazbinsek, Peter Gunter, *J.Mater.Chem*. 2006, 16, 2839-2842.

29 Z.Yang, M. Jazbinsek, B.Ruiz, S. Aravazhi, V. Gramlich, P.Gunter, *Chemistry of Materials.*2007, 19, 3512-3518.

30 Junko Ogawa, Shuji Okada, Zornitza Glavcheva, Hachiro Nakanishi, *J Cryst. Growth.* 2008, 310, 836–842.

31 B. Ferguson, X.C. Zhang, *Nat. Mater*.2002, *1*, 26.

32 O.P. Kwon, S.J. Kwon, M. Jazbinsek, F.D.J.Brunner, J.I. Seo, Ch. Hunziker, A. Schneider, H. Yun, Y.S. Lee, P. Gunter, *Adv. Funct. Mater*., 2008, 18, 3242.

33 O. P. Kwon, S.J. Kwon, M. Stillhart, M. Jazbinsek, A. Schneider, V. Gramlich,P. Gunter, *Cryst. Growth Des*., 2007, 7, 2517.

34 S.J.Kwon, Ch. Hunziker, O.P. Kwon, M. Jazbinsek, P. Gunter, *Cryst. Growth Des.,* 2009, 9, 2512.

35 Jae-Hyeok Jeong, Bong-Joo Kang, Ji-Soo Kim, Mojca Jazbinsek, Seung-Heon Lee, eung-Chul Lee, In-Hyung Baek, Hoseop Yun, Jongtaek Kim, Yoon Sup Lee, Jae-Hyeok Lee, Jae-Ho Kim,Fabian Rotermund& O-Pil Kwon, Scientific Reports, 2013, 3 : 3200.

36 N.P. Rajesh, K. Meera, K. Srinivasan, P. Santhana Raghavan, P. Ramasamy, *J Cryst. Growth.* 2008*, 213, 3*89-394.

37 A. Ioffe, F. Phys. *Status Solidi*, 1989, *116*, 457.

38 N. Vijayan, S. Rajasekaran, G. Bhagavannarayana, R. Ramesh Babu, R. Gopalakrishnan, M Palanichamy, P. Ramasamy, *Crystal Growth & Design*, 2008, 6.

39 K. Jaganathan, S. Kalainathan, *Mater. Res. Bull.*, 2007, 42, 1881-1887.

40 By O-Pil Kwon, Seong-Ji Kwon, Mojca Jazbinsek, D.J. Fabian, Brunner, Jung-In Seo, Christoph Hunziker, Arno Schneider, Hoseop Yun, Yoon-Sup Lee, Peter Gunter, *Adv. Funct. Mater.,* 2008, 18, 3242–3250.

41 Z.Yang, S. Aravazhi, A. Schneider, P. Seiler, M. Jazbinsek, P.Gunter, *Adv. Funct. Mater.*, 2005, 15, 1072-1076.

42 S.Kasap, P. Capper, *Springer Handbook of Electronic and Photonic Materials, Springer Science Inc.*, 2006, 983–996.

43 D.A.Skoog, *Principles of Instrumental Analysis*, first ed., Holt, Rinehart and Winston, New York, 1971.

44 H.H.Willard, L.L. Merritt Jr, J.A.Dean, F.A.Settle Jr, *Instrumental Methods of Analysis, sixth ed.*, Wadsworth Publishing Company, USA, 1986.

45 Z.Glavcheva, H.Umezawa, Y. Mineno, T.Odani, S. Okada, S.Ikeda, T. Taniuchi, H. Nakanishi, *Jpn. J. Appl. Phys.,*2005, 3231.

46 J.Jerald Vijay, N.Melikechib, Tina Thomas, R. Gunaseelan, M. Antony Arockiaraja, P. Sagayaraj, *J. Cryst. Growth,* 2012,338, 170-176.

Caption of the Tables

Table 1. Comparison of lattice parameters value of pure and additive added DSNS.

Lattice parameters	Present work			Reported work[28]
	Pure DSNS	STPB added DSNS	DTPA added DSNS	
Crystal system	Triclinic	Triclinic	Triclinic	Triclinic
Space group	P1	P1	P1	P1
a (Å)	7.887±0.0012	7.846±0.009	7.849±0.001	7.864
b (Å)	8.145±0.001	8.120±0.014	8.144±0.010	8.054
c (Å)	9.910±0.0008	9.911±0.015	9.900±0.010	9.893
α (deg)	69.355±0.005	69.124±0.012	69.182±0.015	70.04
β (deg)	73.234±0.011	72.922±0.008	72.923±0.0013	73.31
γ (deg)	84.212±0.014	84.023±0.003	84.091±0.002	83.69
Volume ($Å^3$)	571.4±0.1	564.3±0.4	567.3±0.2	564.1

Table 2 Comparison of density of pure and additive added DSNS with theoretical density.

S.No	Density of grown crystal by floatation method (g/cc)	Theoretical density of DSNS (g/cc) (from crystallography data)
1	Pure DSNS crystal :1.307	1.314
2	STPB (50 ppm) added DSNS crystal:1.310	
3	DTPA (50 ppm) added DSNS crystal:1.300	

Table 3. Comparison of λ_{max} Values of stilbazolium derivatives.

Crystal [39]	**λ_{max} [a]**
DSHS	474± 1
DSMAS	474± 1
DAST	475± 1
DSMOS	476± 1
DSAS	476± 1
DSNS	**Present work**

[a] In methanol in room temperature

Table 4. Comparative of melting point of stilbazolium derivatives

Crystal	**Melting point (°C)**	**References**
DAST	256± 1	(29)
DSMAS	256± 1	(41)
DSTMS	258± 1	(29)
DSANS	263± 1	(29)
DSMOS	264± 1	(41)
DSDMS	267± 1	(29)
DSAS	272± 1	(41)
DSSS	277± 1	(46)
DASC	281± 1	(45)
DSNS	300± 1	**Present work**

Scheme 1. Synthesis of DSNS

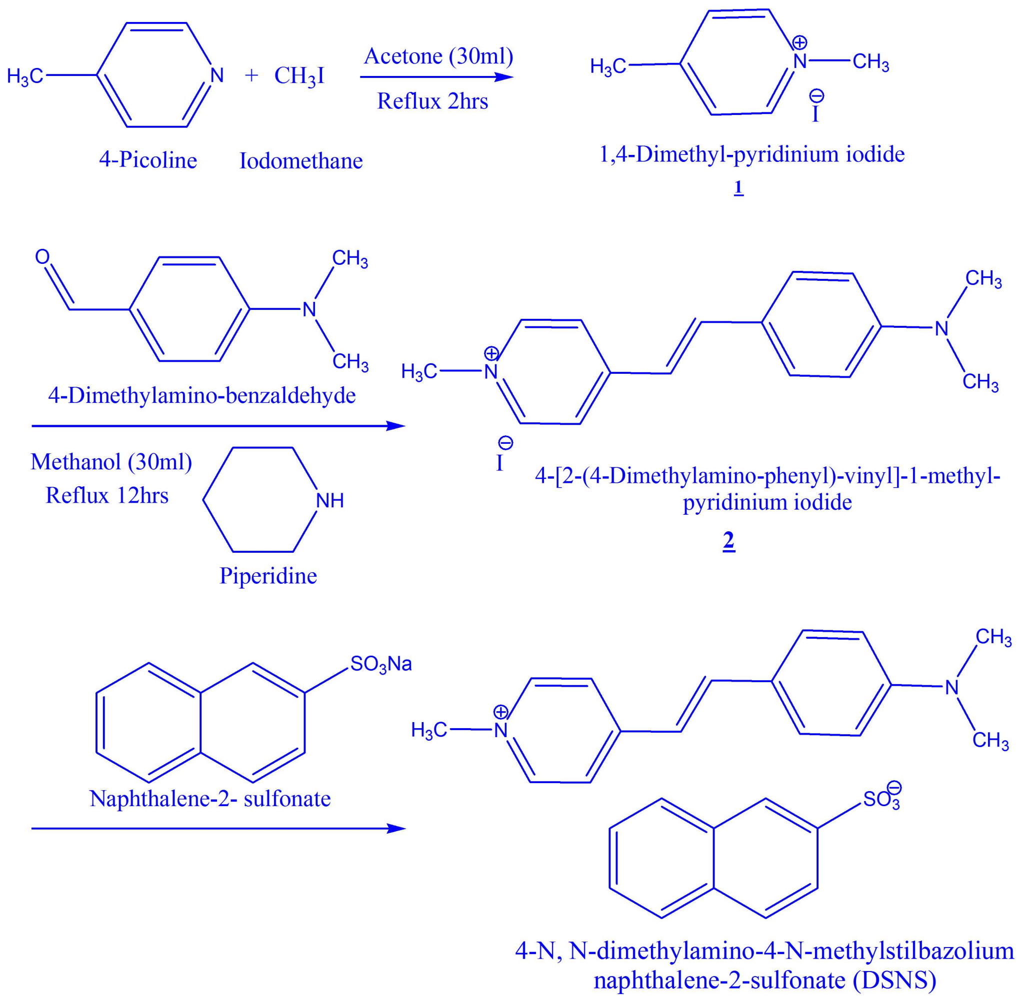

Chart 1. Molecular structure of the STPB and DTPA.

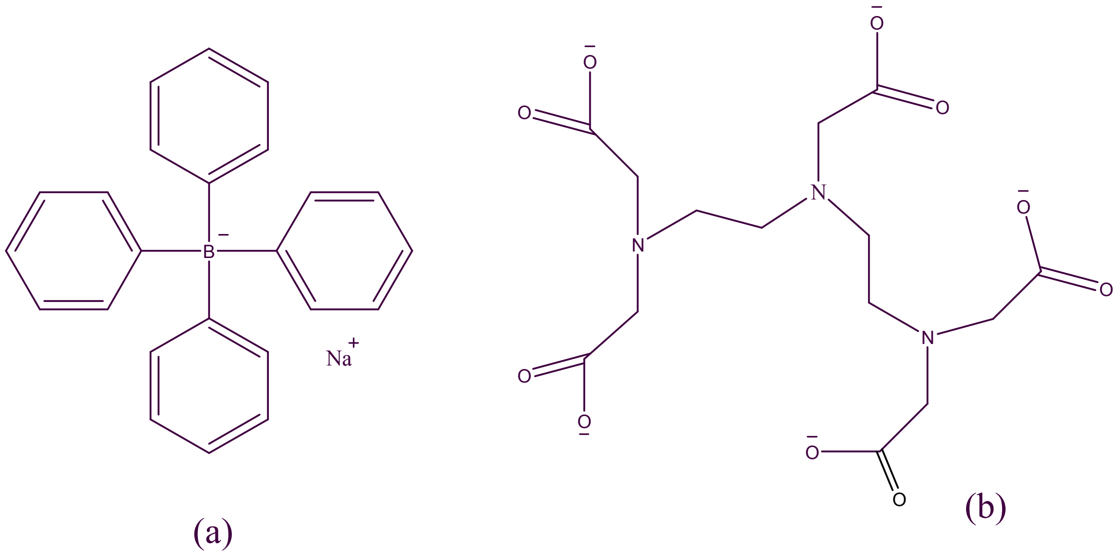

Caption of the Figures

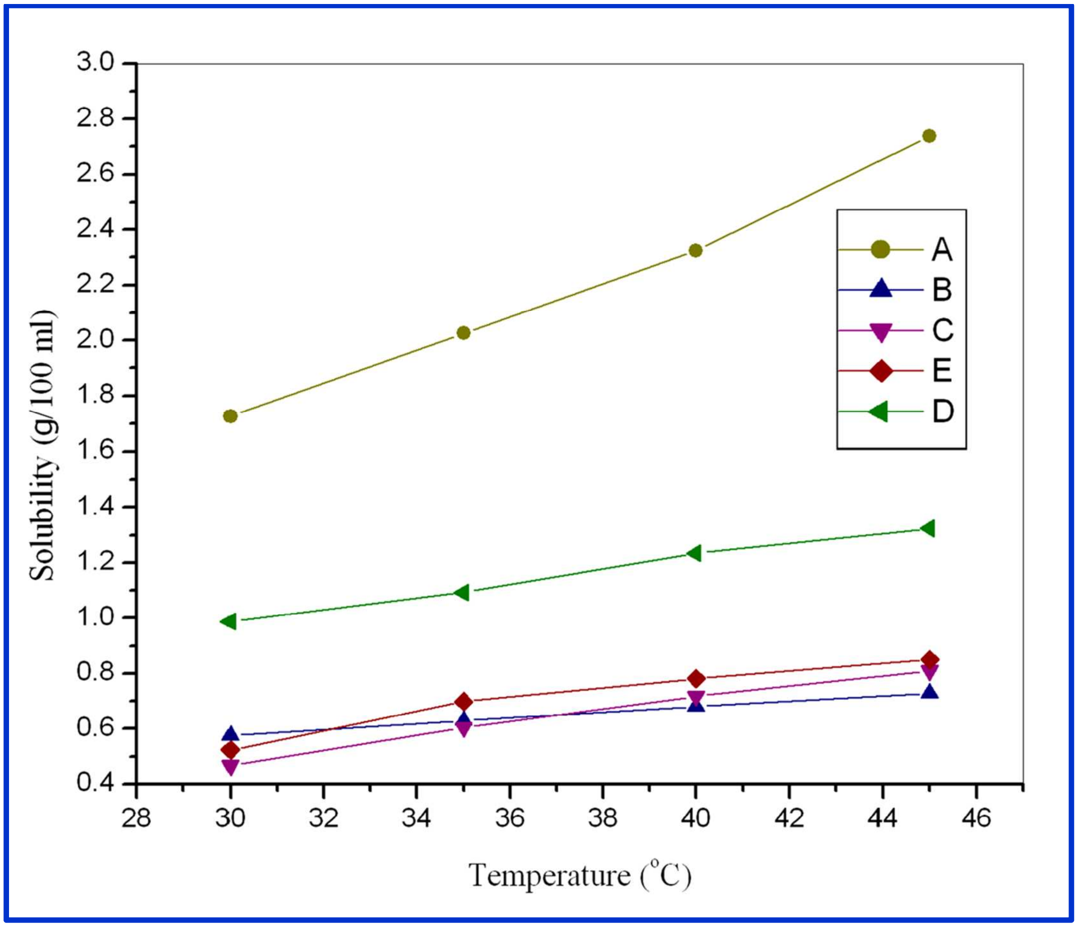

Figure 1. Solubility of DSNS: **A**-Methanol-Chloroform (1:2), **B**-Methanol-Water (9:1), **C**-Methanol-DMF (9:1), **D**-Methanol-Acetonitrile (1:1), **E**-Methanol-DMSO (9:1).

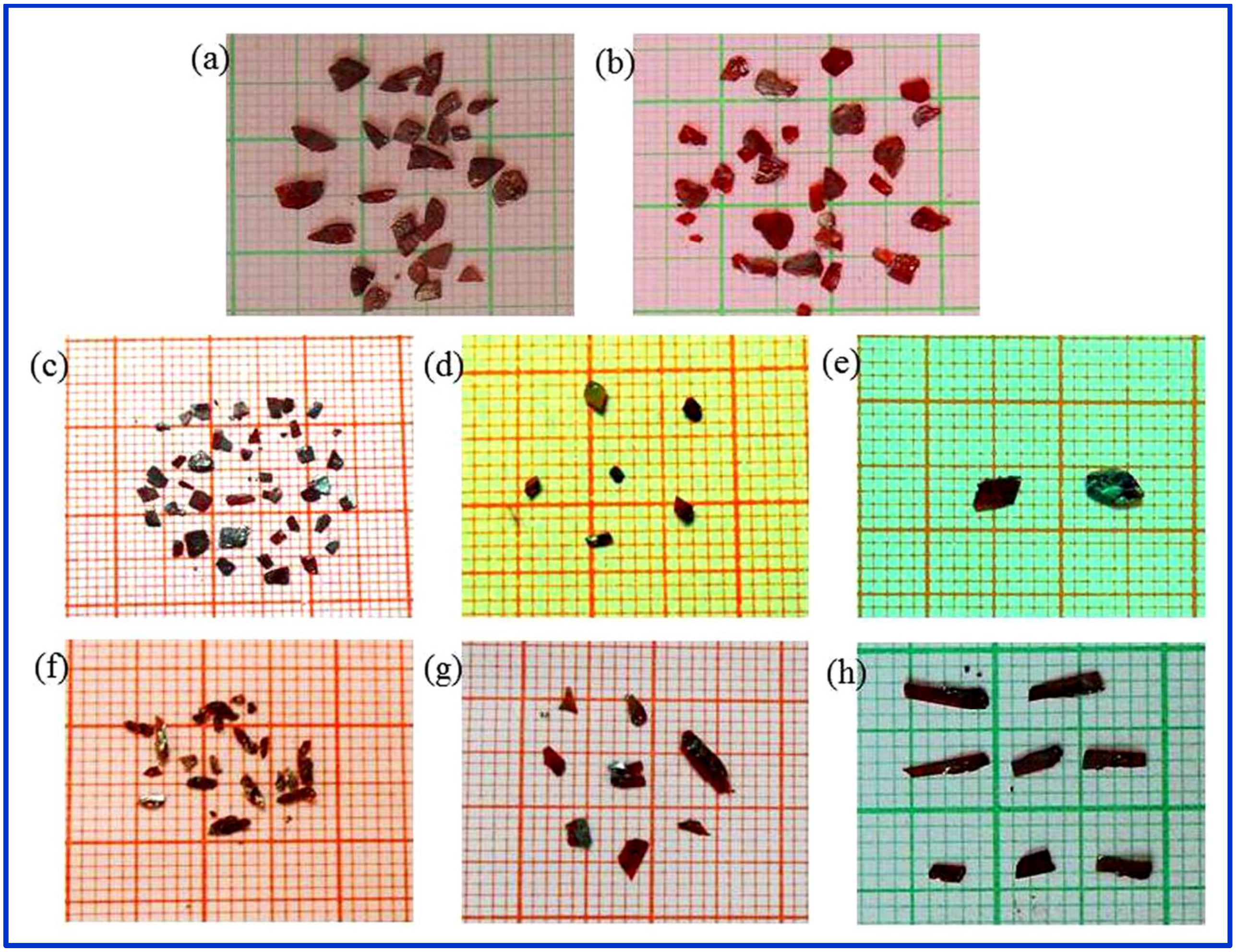

Figure 2.(a) and (b) DSNS crystals grown by slow evaporation method from the pure DSNS solution prepared at 45°C by using mixed solvent system (methanol:DMSO (9:1)) and (b) methanol:DMF (9:1). STPB and DTPA concentrations. (c) STPB-20 ppm, (d) STPB-30 ppm, (e) STPB-50 ppm, (f) DTPA-20 ppm, (g) DTPA-30 ppm, (h) DTPA-50 ppm.

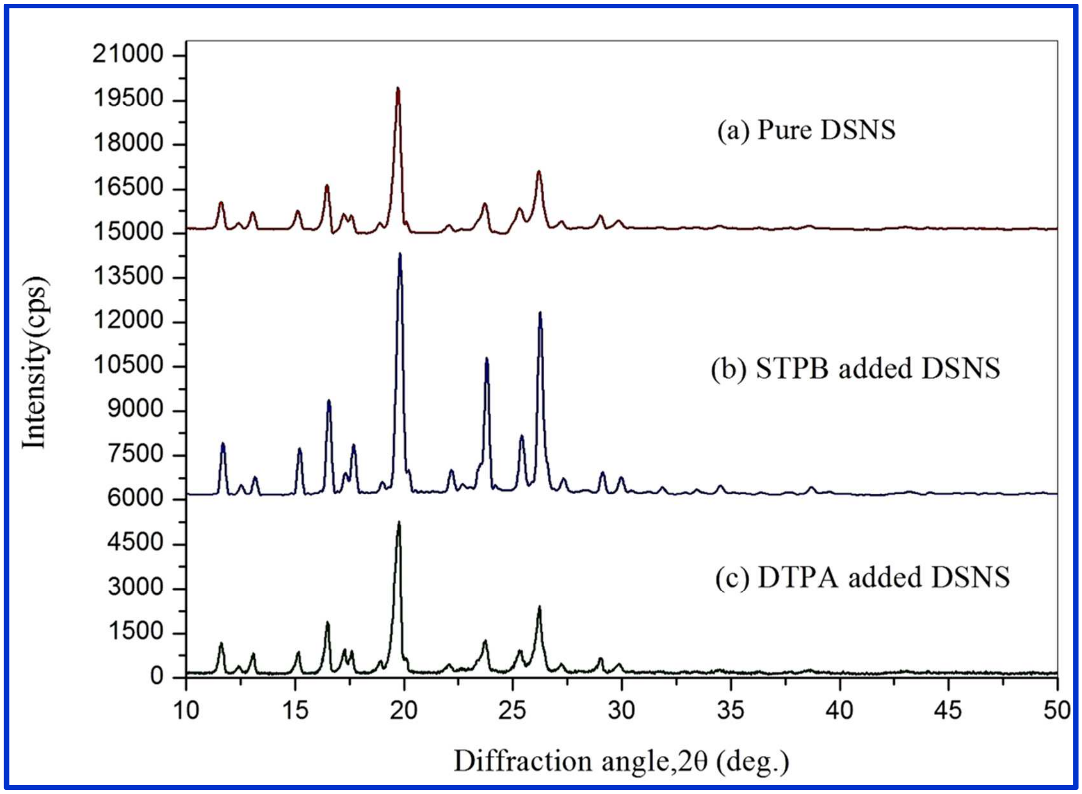

Figure 3. Powder X-Ray Diffraction pattern observed for (a) Pure DSNS and (b) 50ppm STPB added DSNS and (c) 50ppm DTPA added DSNS.

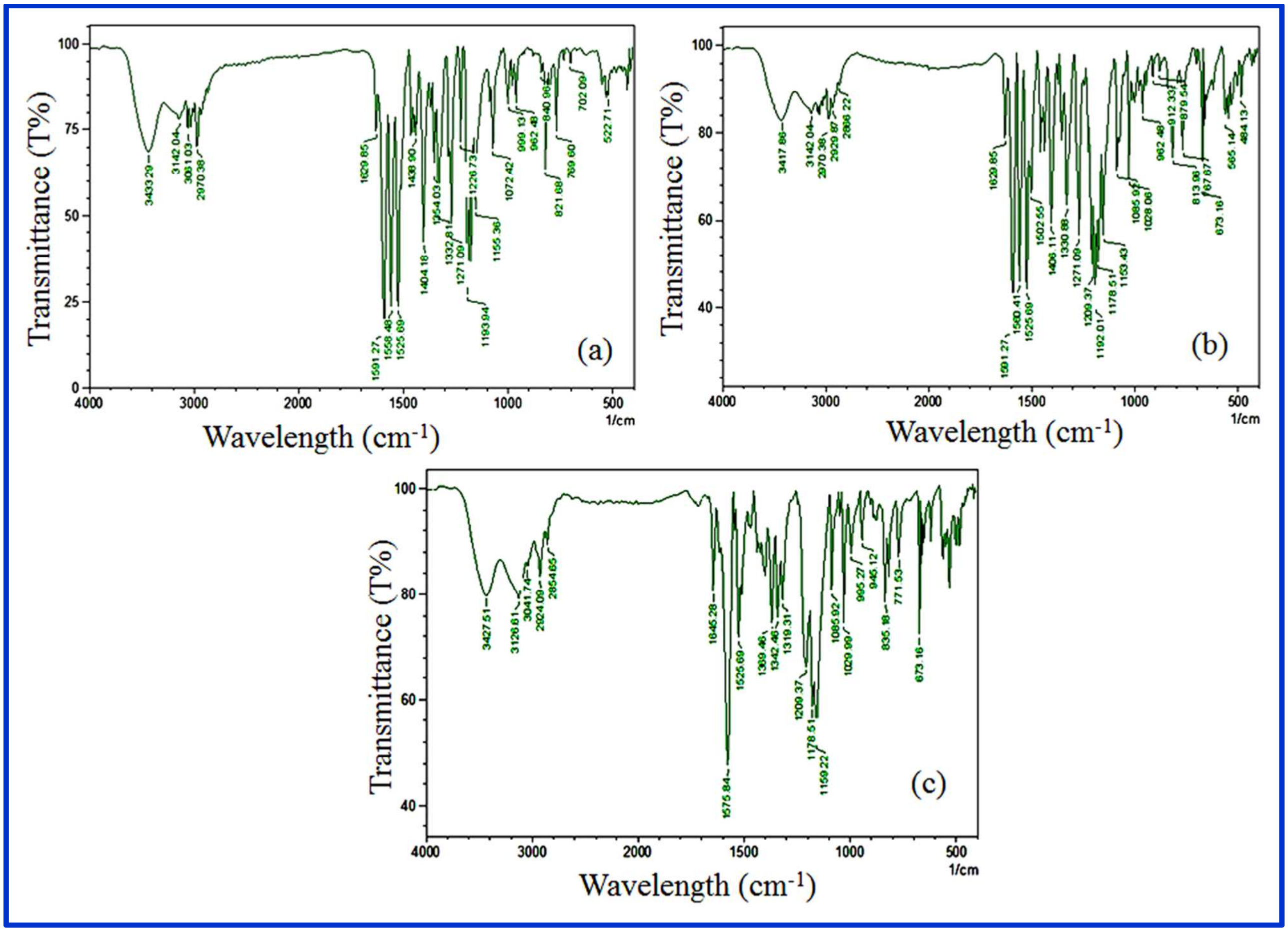

Figure 4. FT-IR Spectrum of (a) pure DSNS and (b) 50 ppm STPB added DSNS and (c) 50ppm DTPA added DSNS crystal.

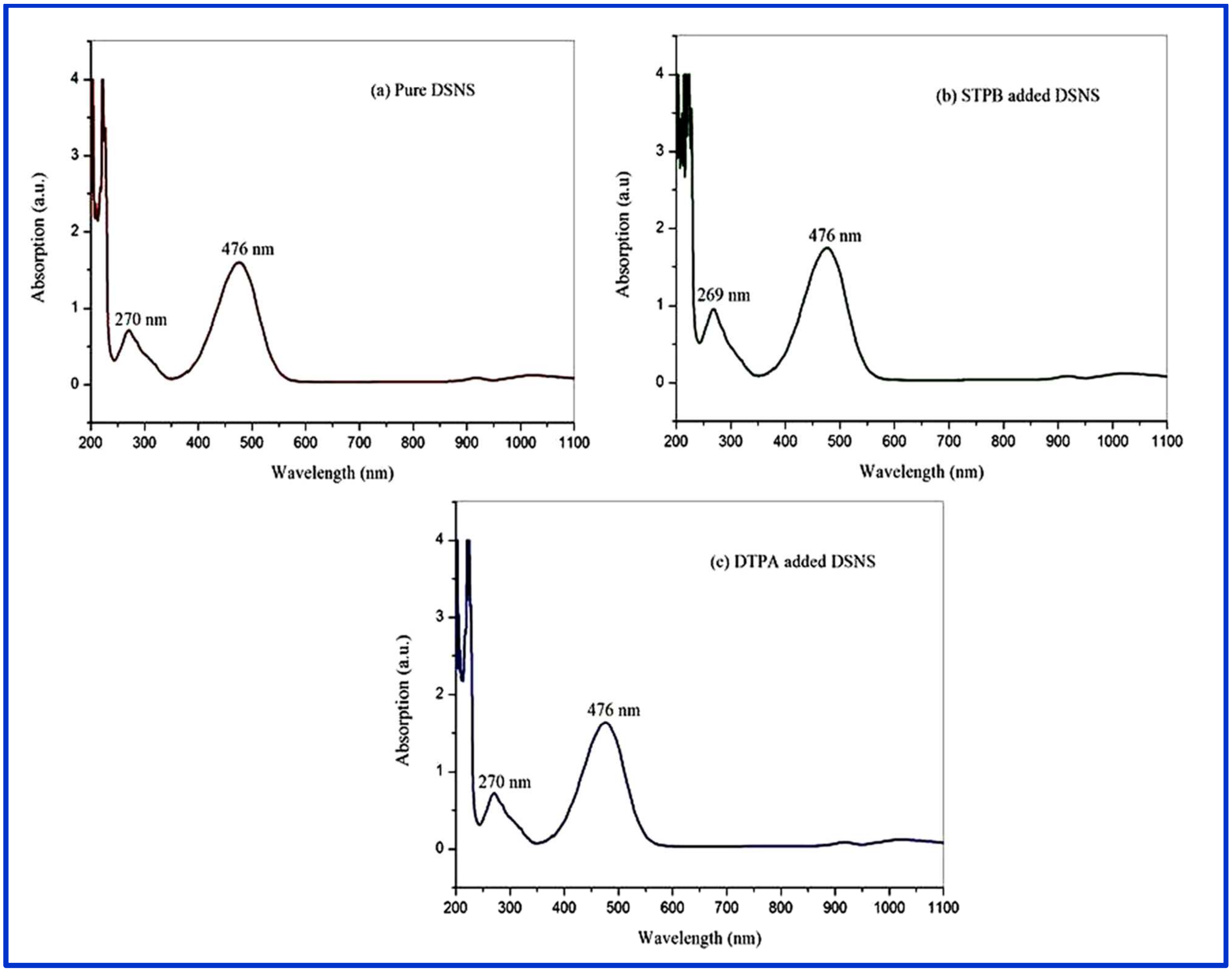

Figure 5. UV-Vis-NIR Spectrum of (a) pure DSNS, 50 ppm STPB added DSNS and 50ppm DTPA added DSNS crystal.

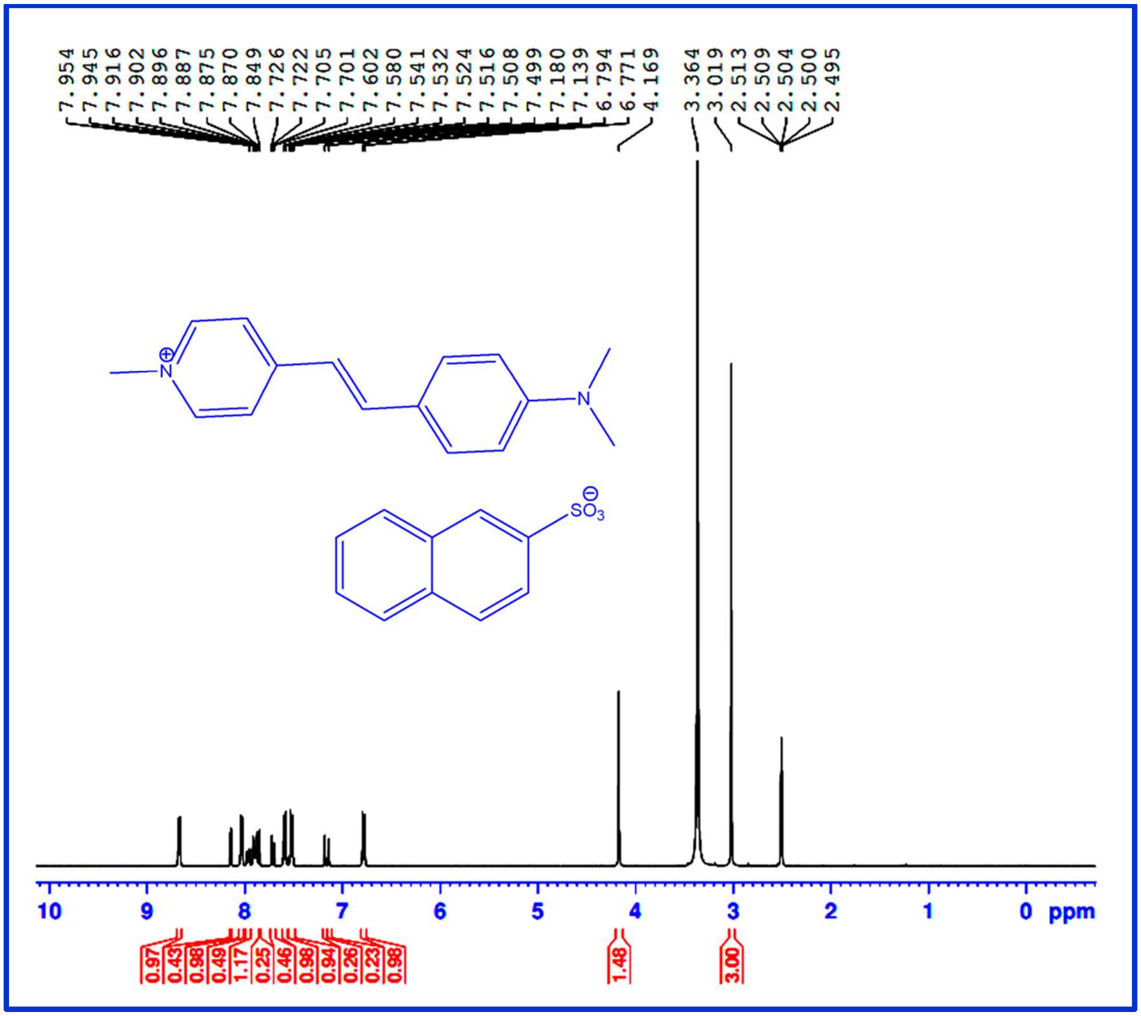

Figure 6. ^{1}HNMR Spectrum of Pure DSNS.

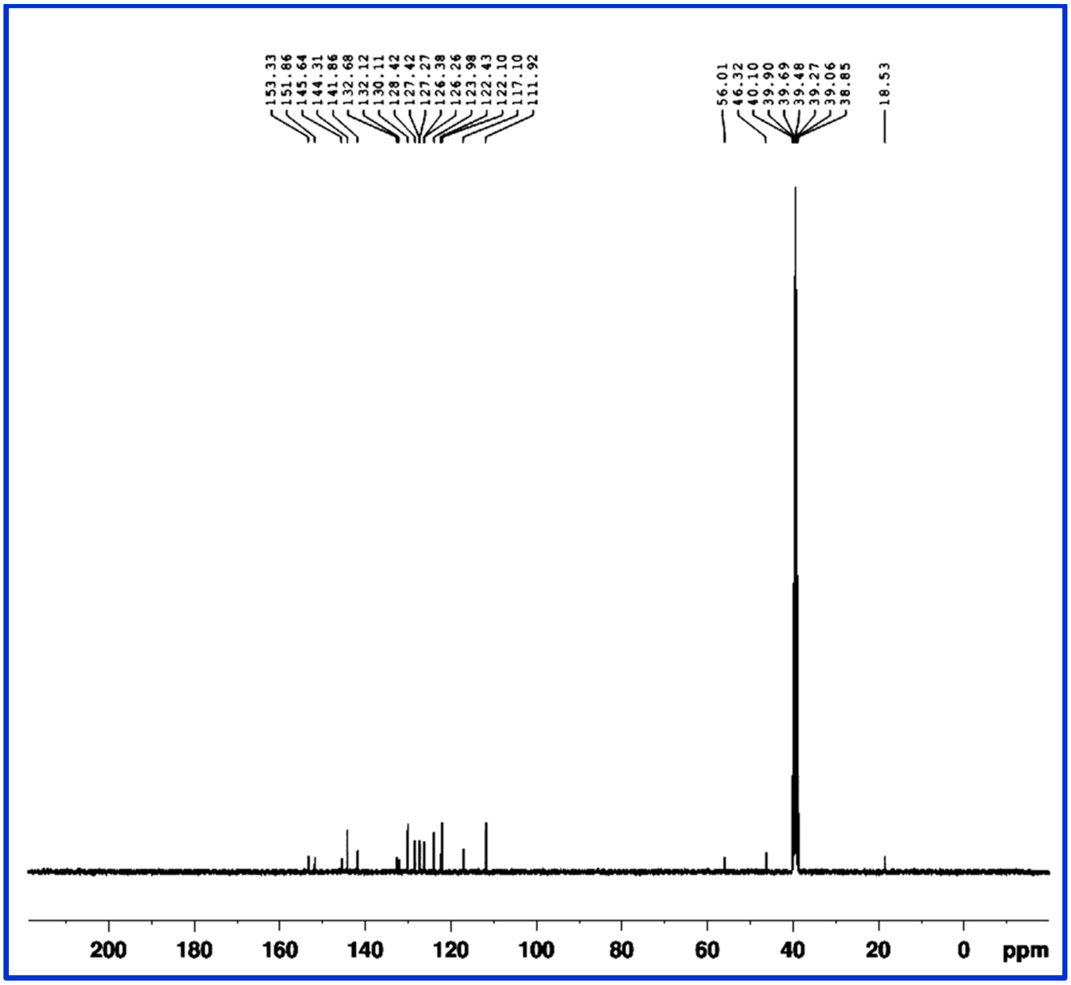

Figure 7. ^{13}C NMR spectrum of Pure DSNS.

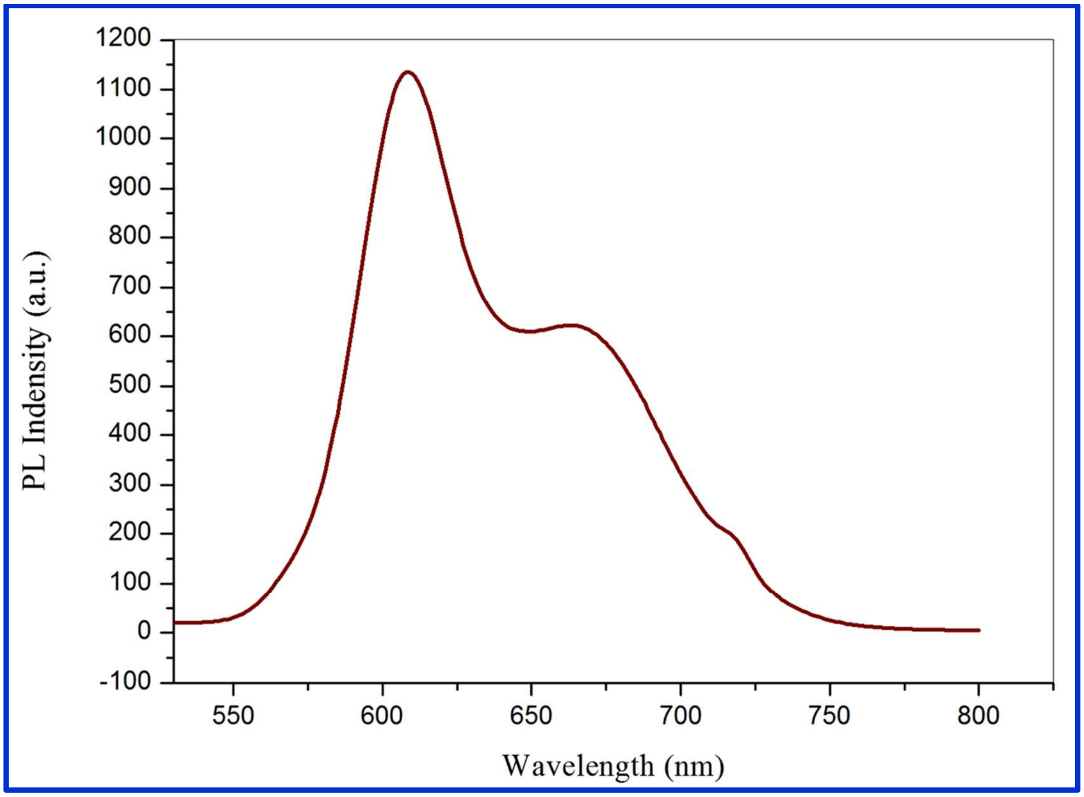

Figure 8. Photoluminescence spectrum of pure DSNS.

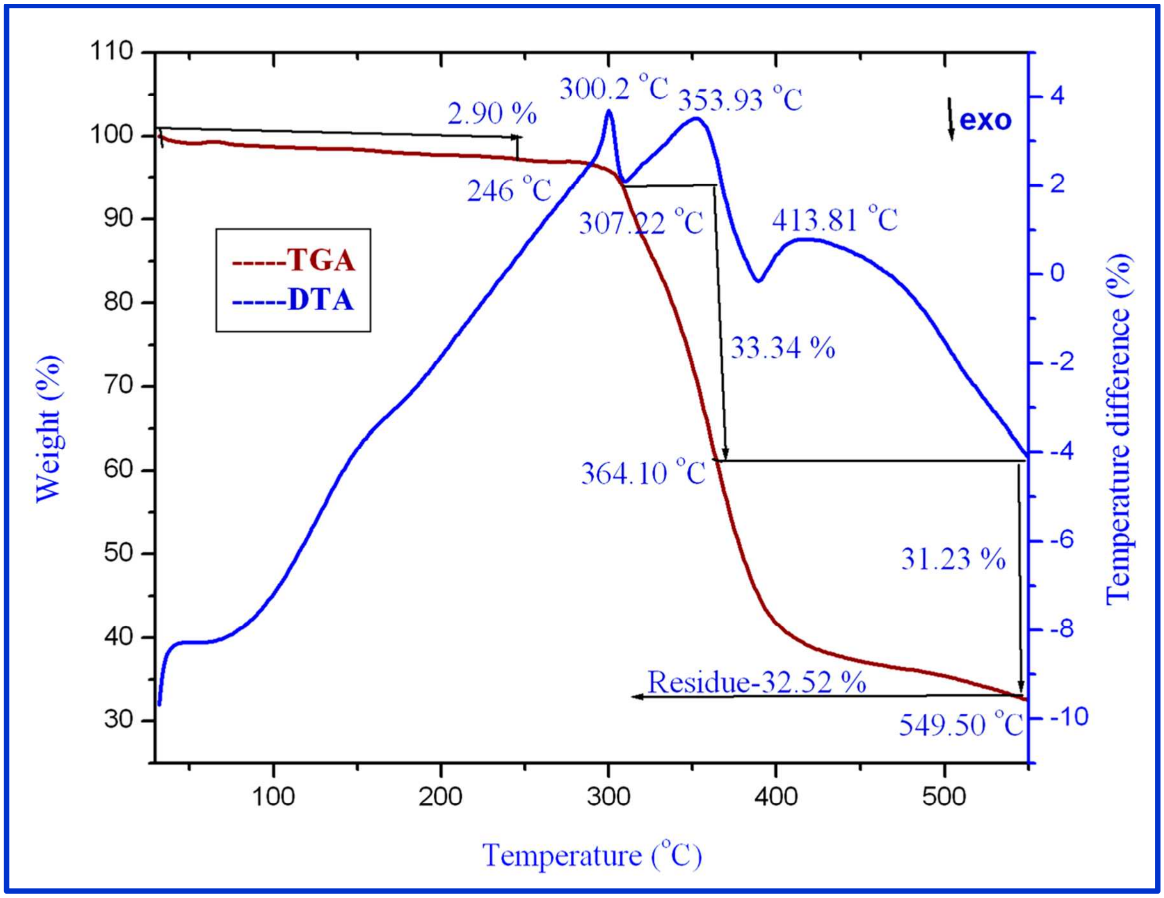

Figure 9. TG-DTA Curve of DSNS.

Graphical Abstract